α_s determination and test of QCD models at various CM energies with L3

Jorge Casaus[a], for the L3 Collaboration.

[a]Unidad de Física de Partículas, CIEMAT,
Avda. Complutense 22, 28040 Madrid, Spain.

We present a study of hadronic events collected by the L3 detector at centre of mass energies around 91 and 133 GeV. Also using hadronic events with a hard radiated photon we obtain a sample at a reduced CM energy of the hadronic system. This will enable us to study event shape variables and determine the strong coupling constant α_s in the range between 30 and 133 GeV. The results presented here are in good agreement with QCD models and the energy dependence of α_s is consistent with expectations of QCD.

1. INTRODUCTION

The basic free parameter of the theory of strong interactions (QCD) [1] is the coupling constant α_s. The nonabelian nature of QCD requires that α_s decreases with increasing energy. In particular, this property is reflected in the energy dependence of the global structure of the hadronic final states in e^+e^- annihilation.

Several experiments have reported α_s measurements as well as studies of event shape variables and comparison with hadronization models in e^+e^- annihilations at different centre of mass energies ranging from 10 to 133 GeV [2].

LEP has produced e^+e^- annihilations at $\sqrt{s} =$ 91 GeV and $130 - 136$ GeV (at the end of 1995). The data collected by the L3 detector has been used for comparing the energy dependence of the mean values of event shape variables as well as for α_s determination at these two energy points.

Furthermore, the high statistics collected by L3 at $\sqrt{s} = 91$ GeV during the period 1991 to 1994 allows us to select samples of hadronic Z decays containing isolated high energy photons. The high energy photons are radiated either by the incoming leptons or through an early branching in the quark bremsstrahlung. The development of the hadronic shower takes place over a larger time scale. So one can effectively look at hadron production at a reduced centre of mass energy from a study of $q\bar{q}\gamma$ events.

We compare the measured distributions of event shape variables at the different effective centre of mass energies ranging from 30 to 136 GeV with theoretical models based on leading log approximation QCD (Parton Shower models) which differ in the variables they use for the leading logarithmic expansion of the cross section and also in the modelling of the hadronization effects. The measured distributions have been compared to the predictions of a second order QCD calculation with resummed leading and next-to-leading terms. This provides determinations of strong coupling constant α_s at several centre of mass energies.

2. THE L3 DETECTOR

The L3 detector consists of a silicon microvertex detector, a central tracking chamber, a high resolution electromagnetic calorimeter composed of BGO crystals, a barrel of scintillation counters, a uranium hadron calorimeter with proportional wire chamber readout, and an accurate muon chamber system. These detectors are installed in a 12 m diameter magnet which provides a solenoidal field of 0.5 T and a toroidal field of 1.2 T. Luminosity is measured with a forward-backward BGO calorimeter on each side of the detector. A detailed description of each detector subsystem and its performance is given in [3,4].

The response of the L3 detector is modelled with GEANT 3.15 [5] detector simulation program which includes the effects of energy loss, multiple scattering and showering in the detector materials and in the beam pipe.

3. EVENT SELECTION

3.1. $q\bar{q}$ selection at $\sqrt{s} = 91$ GeV

We use events collected at a centre of mass energy of $\sqrt{s} = 91.2$ GeV from the 1991 LEP running period, corresponding to an integrated luminosity of about 8 pb^{-1}. Events of type $e^+e^- \to$ hadrons are selected with high efficiency and purity at energies around the Z peak by requiring well balanced events with high calorimetric or track multiplicity and visible energy close to $\sqrt{s}$.

We select 240K hadronic events. The background, arising from $\tau^+\tau^-$ and e^+e^- + hadronic final states, is estimated to be less than 0.2% [6].

3.2. $q\bar{q}$ selection at $\sqrt{s} \simeq 133$ GeV

We use events collected at centre of mass energies of $\sqrt{s} = 130.3$ and 136.3 GeV from the 1995 LEP high energy run, corresponding to a total integrated luminosity of 5 pb^{-1}. The hadronic events are selected using similar cuts as described above.

The fraction of events with hard initial state radiation (ISR) in the hadronic sample is about 75%. In order to reduce this contamination, we try to reject events arising from an ISR photon lost in the beam pipe using their lower visible energy as well as their larger longitudinal imbalance along the beam axis. The well balanced events could contain initial state radiation where the photon is seen in the detector. These are removed requiring that the energy of the most energetic photon candidate should be less than 15 GeV.

We select 241 and 161 hadronic events for the 130 and 136 GeV samples respectively. After all the cuts, the contamination from hard ISR (γ energy greater than 15 GeV) amounts to about 20% of the sample. The effect of ISR on the mean effective centre of mass energy is accounted for using Monte Carlo. The remaining background, due e^+e^- + hadronic final states, is estimated to be less than 2% [7].

3.3. $q\bar{q}$ selection at $\sqrt{s'} < M_Z$

We use events collected at $\sqrt{s} \simeq 91$ GeV from 1991 to 1994, corresponding to a luminosity of 111 pb^{-1}. After applying the cuts described in section 3.1 we select 2990 K hadronic events.

We select hadronic events containing photon candidates identified in the electromagnetic calorimeter. The energy distribution of the photons, E_γ, can be translated into the energy distribution of the remaining hadronic system, $\sqrt{s'}$, using the expression

$$\sqrt{s'} = \sqrt{s \cdot \left(1 - \frac{2E_\gamma}{\sqrt{s}}\right)}. \qquad (1)$$

The $\sqrt{s'}$ spectrum spans from 30 to 86 GeV. We have divided it into six bins so that each one contains reasonable statistics.

The background to direct photons is dominated by photons coming from π^o and η decays. To reduce this background, we require that the photon candidate should be isolated and that the shower shape is compatible with single γ electromagnetic shower. The absolute rate of this background is not well described in the Monte Carlo and it has been reestimated from the data by selecting a background sample with the same energy and isolation cuts as the γ sample and then comparing with Monte Carlo predictions assuming that the signal part is well described.

We select around 1 K events per $\sqrt{s'}$ bin with an efficiency between 35% and 65% depending on the photon energy whereas the purity is better than 75% at all energies [8].

4. EVENT SHAPE VARIABLES AND CORRECTIONS

The event shape variables used in the analysis are: event thrust, T [9], scaled heavy jet mass, $\rho = M_H^2/s$ [10], total and wide jet broadening, $B_{T,W}$ [11].

The distributions are measured from calorimetric clusters using histograms with bin widths bigger than the experimental resolution. In the case of $q\bar{q}\gamma$ selection, the variables are calculated after boosting the event in the CM frame of the hadronic system using the well measured energy and angle of the isolated photon.

The backgrounds are subtracted on a bin-by-bin basis and the effect of detector resolution, acceptance and initial and final state radiation have been taken into account using Monte Carlo.

Table 1
Mean values of thrust, T, scaled heavy jet mass, ρ, total jet broadening, B_T, and wide jet broadening, B_W, measured as various CM energies. Statistical and systematic errors have been added in quadrature.

$\sqrt{s}$ (GeV)	$<T>$	$<\rho>$	$<B_T>$	$<B_W>$
30–50	0.906 ± 0.005	0.065 ± 0.003	0.139 ± 0.003	0.088 ± 0.004
50–60	0.917 ± 0.004	0.061 ± 0.004	0.127 ± 0.003	0.083 ± 0.004
60–70	0.922 ± 0.004	0.059 ± 0.002	0.120 ± 0.004	0.081 ± 0.004
70–80	0.928 ± 0.003	0.051 ± 0.002	0.113 ± 0.002	0.075 ± 0.005
80–84	0.929 ± 0.004	0.051 ± 0.002	0.112 ± 0.004	0.075 ± 0.005
84–86	0.932 ± 0.005	0.050 ± 0.003	0.109 ± 0.005	0.073 ± 0.006
91	0.936 ± 0.002	0.054 ± 0.001	0.110 ± 0.002	0.074 ± 0.002
130	0.948 ± 0.008	0.045 ± 0.003	0.095 ± 0.004	0.067 ± 0.003
136	0.943 ± 0.009	0.046 ± 0.004	0.094 ± 0.005	0.066 ± 0.004

The experimental errors for the analysis at $\sqrt{s} = 91$ GeV are estimated by varying the energy response of the calorimeters, comparing the distributions unfolded using simulated JETSET [12] and HERWIG [13] events and comparing the corrected distributions obtained from calorimetric clusters and charged tracks. The systematic uncertainties are the main contribution to the total experimental error.

In the case of the analysis of the sample obtained at $\sqrt{s} \simeq 133$ GeV, the dominant systematic uncertainty comes from correction due to initial state radiation and it has been estimated comparing the result obtained with all the cuts with the result obtained after removing the cut on the visible photon in the detector. The total experimental errors are dominated by the statistical error of the data sample.

The systematic errors in the analysis of the $q\bar{q}\gamma$ sample are dominated by the uncertainty in the background scale factors, the dependence on the correction methods and the effect of the variation of selection cuts. The systematic uncertainties are of the same order as the statistical errors.

5. COMPARISON WITH QCD MODELS

An important test of the QCD models is to check the predicted energy evolution of the event shape distributions.

The measured mean values of thrust, scaled heavy jet mass, total and wide jet broadening at the different centre of mass energies are summarized in table 1. Figure 1 shows the energy evolution of these values compared to the predictions from ARIADNE 4.06 [14], HERWIG 5.8 [13] and JETSET 7.4 PS [12]. Events have been generated using a parameter set tuned with the L3 data at the Z peak [15] and the initial and final state radiation has been switched off.

The QCD models agree with the trend in the data over the full energy range.

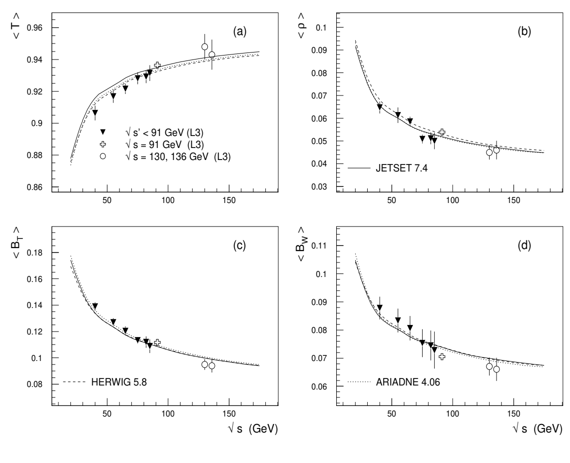

Figure 1. Corrected distributions for mean (a) thrust, T, (b) scaled heavy jet mass, ρ, (c) total jet broadening, B_T, and (d) wide jet broadening, B_W, as a function of CM energy. The smooth lines correspond to the predictions of different QCD models.

6. QCD PREDICTIONS AND α_s MEASUREMENT

QCD predictions in fixed second order perturbation theory are known for all the event shape variables from numerical integration of the exact matrix element [16]. For the variables used in this analysis the leading and next-to-leading logarithmic contributions have been resummed [17]. The theoretical predictions can be improved by a matching of fixed order and the resummed calculations. Nevertheless, the matching prescription is not unique and leads to the so called matching ambiguities [18].

The dependence on the uncalculated higher order corrections is expected to be smaller when using the resummed plus fixed order QCD predictions. On the other hand, the theoretical predictions are reliable over a larger kinematical range.

To compare the analytical calculations with the experimental distributions, we fold the perturbative calculations with the hadronization kernels defined using the parton shower programs JETSET and HERWIG with string or cluster fragmentation. The correction for hadronization and decays changes the perturbative prediction by less than 5% for the event shape variables over a wide kinematic range. The hadronization uncertainties are estimated by changing the fragmentation parameters in the JETSET model and also comparing the predictions of the different hadronization models.

In order to derive α_s, we fit the theoretical distributions for a fixed value of the renormalization scale $\mu = \sqrt{s}$ to the measured event shape distributions over the fit range. The fit range is such that the theoretical calculation is reliable and the detector and hadronization corrections are small.

The uncertainty coming from uncalculated higher orders in the QCD predictions is reflected in the dependence of the fitted α_s value on the renormalization scale μ. The scale error is estimated by repeating the α_s fit for different values of μ in the interval $0.5 \leq \mu/\sqrt{s} \leq 2$. The matching scheme uncertainty is obtained from half the maximum spread due to the variation of the matching algorithm. The systematic uncertainties due to uncalculated higher order terms have been estimated as the largest of scale and matching scheme uncertainty. The overall theoretical error is obtained by adding to this, in quadrature, the hadronization uncertainty. The theoretical uncertainties, which dominate the α_s measurement at $\sqrt{s} = 91$ GeV [6], are of the same order as the experimental errors for the other seven energy points [7,8].

The α_s values from the four distributions are affected differently by higher order corrections and hadronization effects. To obtain a combined value of the strong coupling constant, we take the unweighted average of the four α_s values. The overall experimental error is obtained by adding in quadrature the statistical error and the unweighted average of experimental systematic errors. We assign the overall theoretical uncertainty as the average of the theoretical errors obtained from the four different measurements at each CM energy. The combined results are summarized in table 2. Figure 2 contains the α_s values measured at the different centre of mass energies by L3. The smooth curve on the figure is the QCD expectation for five quark active flavours and $\alpha_s(M_Z) = 0.120$. The energy dependence of α_s is consistent with QCD expectations [1].

Table 2
α_s at the eight CM energies from the four fits to the event shape variables.

$\sqrt{s}$ (GeV)	α_s ($\sqrt{s}$)	$\Delta\alpha_s$ (exp.)	$\Delta\alpha_s$ (thy.)
30 – 50	0.139	± 0.010	± 0.009
50 – 60	0.139	± 0.011	± 0.007
60 – 70	0.132	± 0.008	± 0.006
70 – 80	0.116	± 0.008	± 0.006
80 – 84	0.118	± 0.010	± 0.007
84 – 86	0.111	± 0.010	± 0.005
91	0.122	± 0.002	± 0.007
133	0.107	± 0.005	± 0.006

[1] The measurements favour the running of α_s ($\chi^2/\mathrm{dof} = 8.7/7$) against a constant value of the coupling constant ($\chi^2/\mathrm{dof} = 24.7/7$).

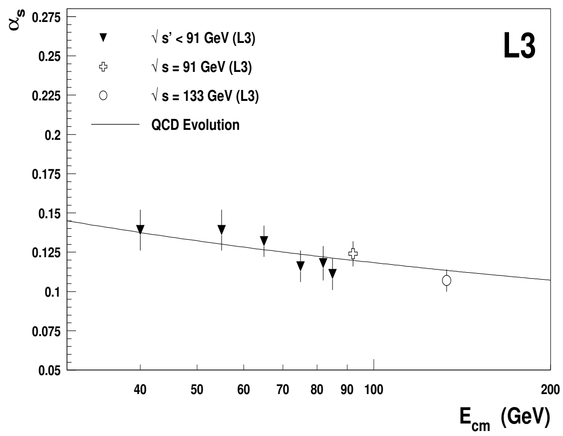

Figure 2. L3 measurements of α_s at various CM energies from event shape variables.

7. CONCLUSIONS

We have studied a number of event shape variables using the sample of hadronic events produced in e^+e^- annihilations at $\sqrt{s} = 91$ and 133 GeV. In addition to that, we have selected hadronic events with isolated photons from Z decays which lead to hadronic systems produced at different reduced CM energies. The resulting distributions are compared with the expectations of several QCD models. Data agree with the energy evolution of the QCD models JETSET 7.4 PS, HERWIG 5.8 and ARIADNE 4.06.

From a fit of the second order QCD calculation with resummed leading and next-to-leading terms to the thrust, scaled heavy jet mass and total and wide jet broadening distributions we determine the strong coupling constant α_s at eight different energy points. The energy dependence of α_s is in good agreement with the QCD expectations.

ACKNOWLEDGEMENTS

I am indebted to my colleagues of the L3 collaboration. In particular, I would like to thank Sunanda Banerjee, Dominique Duchesneau and Subir Sarkar for their help in the preparation of this document.

REFERENCES

1. H. Fritzsch and M. Gell-Mann, *16th Intern. Conf. on High Energy Physics*, Chicago-Batavia (1972); H. Fritzsch, M. Gell-Mann and H. Leutwyler, Phys. Lett. **B47** (1973) 365; D.J. Gross and F. Wilczek, Phys. Rev. Lett. **30** (1973) 1343; H.D. Politzer, Phys. Rev. Lett. **30** (1973) 1346.
2. S. Bethke, these proceedings.
3. L3 Coll., O. Adriani *et al.*, Phys. Rep., **236** (1993) 1.
4. L3 Coll., B. Adeva *et al.*, Nucl. Inst. Meth. **A289** (1990) 35; L3 Coll., M. Acciari *et al.*, Nucl. Inst. Meth. **A351** (1994) 300.
5. The L3 detector simulation is based on GEANT 3.15. See R. Brun *et al.*, "GEANT 3", CERN DD/EE/84-1 (Revised), September 1987.
6. L3 Coll., O. Adriani et al., Phys. lett. **B284** (1992) 471; L3 note # 1441, July 1993.
7. L3 Coll., M. Acciarri et al., Phys. lett. **B371** (1996) 137.
8. L3 note # 1958, June 1996, *Contribution to ICHEP 96.*
9. E. Fahri, Phys. Rev. Lett. **39** (1977) 1587.
10. T. Chandramohan and L. Clavelli, Nucl. Phys. **B184** (1981) 365.
11. S. Catani, G. Turnock and B.R. Webber, Phys. Lett. **B295** (1992) 269.
12. JETSET 7.4: T. Sjöstrand and M. Begtson, Comp. Phys. Comm. **43** (1987) 367.
13. HERWIG 5.8: G. Marchesini and B.R. Webber, Nucl. Phys. **B310** (1988) 461.
14. ARIADNE 4.06: U. Pettersson, LUND Preprint, LU TP 88-5
15. L3 Coll., B. Adeva *et al.* , Z. Phys. **C55** (1992) 39.
16. R.K. Ellis, D.A. Ross and A.E. Terrano, Nucl. Phys. **B178** (1981) 421.
17. S. Catani, G. Turnock, B.R. Webber and L. Trentadue, Phys. Lett. **B263** (1991) 491; S. Catani, G. Turnock and B.R. Webber, Phys. Lett. **B272** (1991) 368; S. Catani, G. Turnock and B.R. Webber, Phys. Lett. **B295** (1992) 269.
18. S. Catani, L. Trentadue and G. Turnock and B.R. Webber, Nucl. Phys. **B407** (1993) 3.